11;10.2

Effect of the polarization of satellite navigation antennas on multipath error envelopes

© A.A. Erokhin, E.R. Gafarov, A.M. Alexandrin, R.O. Ryazantsev, S.V. Polenga, Yu.P. Salomatov

Siberian Federal University, Krasnoyarsk, Russia
E-mail: aerokhin@sfu-kras.ru

Received May 16, 2022
Revised October 24, 2022
Accepted October 25, 2022

The paper estimates the envelope of error introduced by the effect of multipath propagation in global navigation satellite systems. Based on the mathematical model of the radio path of the direct and reflected signals, the results of the multipath error envelopes for various types of navigation antennas are obtained.

Keywords: antenna, GNSS, multipath interference, interference, radiation pattern, multipath error envelope.

DOI: 10.21883/TPL.2022.12.54952.19249

The ground-based segment of the global navigation satellite systems (GNSS) such as GPS, GLONASS, etc., possesses at present an acute problem of the multipath interference (MI). As papers [1,2] report, MI reduces the accuracy of positioning because an GNSS antenna receives both the direct (desired) and reflected (interference) signals. The interference signal emerges due to reflection from the underlying relief around the antenna. As a rule, the interference signal always exists during receiving the direct signal from the satellite; however, there are available methods for preventing MI, which may be realized in the antenna itself: 1) polarization selection; 2) spatial selection. Therefore, the goal of this study was determining the influence of various-type antennas on the GNSS positioning accuracy.

It is known [3] that, being reflected, the signal undergoes polarization inversion (for instance, the direct signal is right-circularly polarized, while the reflected one is left-circularly polarized). The polarization selection is realized in the antenna by suppressing the minor-type polarization; in GNSS, this is the left-circular polarization [4].

The spatial selection consists in reducing the radiation at the transition to the non-working angle sector. The sharper is this transition (high slope of the radiation pattern (RP)), the weaker is the interference signal effect on the coordinate-determination error. Ideally, the RP slope is to tend to infinity. For the base station antennas equipped with choke-ring screens [5], suppression of radiation in the non-working angle range is ensured, but the RP slope is about 0.3 dB/deg. In the recent times, cylindrical helical antennas are being studied [6,7], whose RP slope amounts up to 0.7−0.9 dB/deg.

Therefore, of interest is estimation of MI, methods for controlling which are realized in GNSS antennas of various types using spatial characteristics.

For the estimation of antenna influence on the reduction of the MI effect, a mathematical model was created. The model is based on the concept of reflective radio-wave propagation accounting for the Earth sphericity. In the framework of reflective radio-wave propagation concept, the spherical Earth is replaced with the flat one. In this case, a tangent to the spherical Earth surface is drawn at the reflection point (point C in Fig. 1). The tangent represents the flat Earth surface; the reduced distances covered by the direct and reflected waves are calculated relative to it. Similar models of radio-wave propagation intended for estimating the positioning accuracy are used also by other authors (see, e.g., [8]).

It is also necessary to determine the coefficient of reflection from the Earth surface. Assume that dimensions of the upper layer and underlying medium are semi-infinite. As the underlying medium, seawater is taken; its dielectric permittivity was determined by using the model proposed

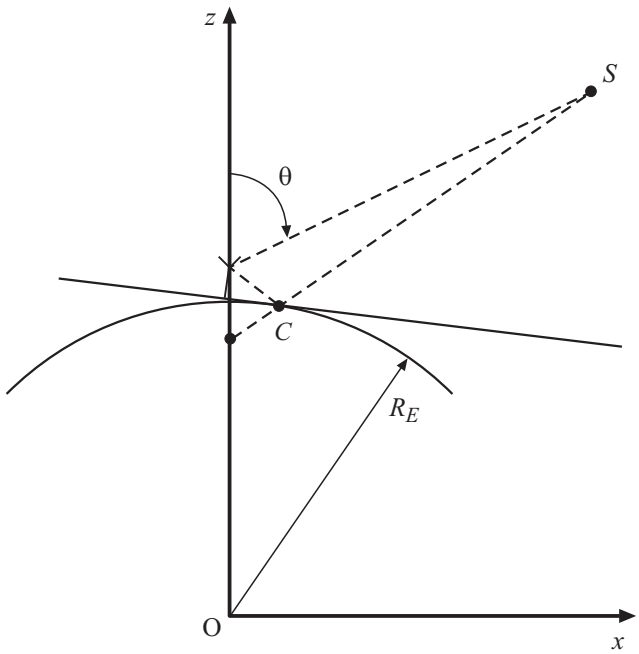

Figure 1. Scheme of the radio wave propagation. S — satellite, C — reflection point, R_E — Earthś radius, θ — radiation pattern angle.

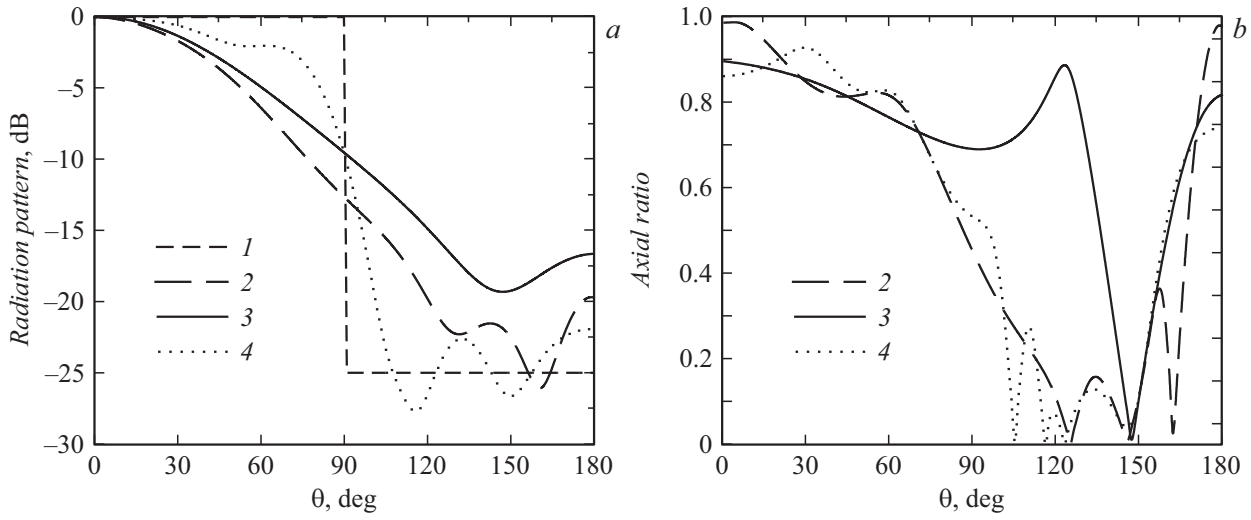

Figure 2. Radiation pattern characteristics: *a* — RP, *b* — ER. *1* — ideal antenna, *2* — choke-ring antenna, *3* — helical-slot antenna, *4* — helical antenna.

in [9]. Reflection coefficients for the left-circular and right-circular polarizations may be written as follows:

$$R_{right} = \frac{1}{\sqrt{2}}(R_v + jR_h), \quad R_{left} = \frac{1}{\sqrt{2}}(R_v - jR_h), \quad (1)$$

where R_v, R_h are the reflection coefficients for the vertical and horizontal polarizations, respectively.

The positioning accuracy may be estimated by using the multipath error envelope [3] that may be expressed in meters and is equal to the pseudo-range estimation error. Sampling rate of the standard-accuracy signal code symbols in the GLONASS system (frequency range L1) is 511 kHz, which causes the multipath error of 14.7 m in receiving the signal by an isotropic antenna (in the case of a single reflection with the coefficient of 0.5; the seawater reflection coefficient is higher: $R_{right}, R_{left} > 0.6$). The multipath error of the standard-accuracy signal is used in comparing antennas of different types.

Let us consider a graphical presentation of the multipath error envelope constructed in the form of the dependence on the GNSS satellite observation angle with accounting for the reflection coefficient (1) and receiving antenna RP. According to [3], the multipath error envelope is represented by a piecewise-linear function whose argument is the delay of the reflected signal relative to the direct one. In the used model, this delay was recalculated into the desired signal acceptance angles. As the receiving antennas, we used a choke-ring antenna about 2λ in size [5], a helical-slot antenna 0.5λ in size [4], or a cylindrical helical antenna 1.8λ in height [6]. As noticed above, those antennas have different RP slopees at the transition to the non-working range of angles and are characterized by different extents of the polarization decoupling, namely, axial ratio (AR). The mathematical model of the multipath error envelope accounts for properties of the polarization and radiation pattern (including the RP slope); this is why it is convenient

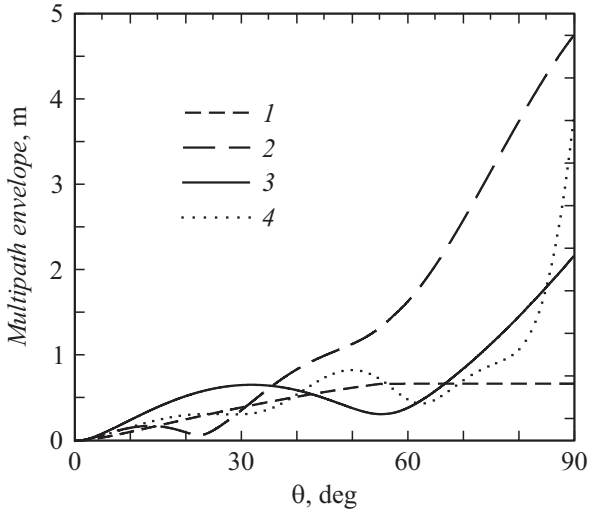

Figure 3. Multipath error envelope. *1* — ideal RP, *2* — choke-ring antenna, *3* — helical-slot antenna, *4* — helical antenna.

for estimation with respect to these two parameters. Fig. 2 illustrates RP via the antenna absolute field and ER at the GLONASS central frequency L1. The obtained results of modeling the multipath error envelope are shown in Fig. 3. In addition, Fig. 3 demonstrates the multipath error envelope for the ideal „rectangular" RP with the width of 180 deg, slope infinite in the towards-horizon direction ($\theta = 90$ deg), and backward radiation level of -25 dB. Notice that the results of using surfaces of other types are qualitatively comparable with those obtained here, while quantitative estimate of the multipath envelope error will be somewhat lower because of a lower reflection coefficient [8].

As the presented curves show, the multipath error becomes significantly higher at the angles of 50 to 90 deg depending on the antenna type. The increase in the multipath error is connected with that the real antenna RP

width is below 180 deg. The ideal RP does not exhibit a sharp increase in the error. In addition, the multipath error is affected also by the antennaś polarization RP that changes from the right polarization in the main lobe to the left one in the side (back) lobe; therefore, the multipath error is non-zero even for the ideal RP.

The RP slopees for real antennas, choke-ring and helical-slot ones, are approximately equal; however, the multipath error of the helical-slot antenna is twice lower due to better polarization decoupling. Notice here that not only multipath interference but also the antenna efficiency factor affects the positioning accuracy. The efficiency decrease is proportional to the decrease in the pseudo-range determination accuracy caused by an increase in the signal/noise ratio. The helical-slot antenna is designed so as to ensure the traveling wave regime in the stripline feeder ending with an absorber; hence, high magnitudes of the polarization decoupling may be achieved by decreasing the efficiency factor (to about 50%).

This disadvantage is not inherent to the cylindrical helical antenna which is characterized by a high efficiency and high RP slope. Due to this, the antenna exhibits a low multipath error that remains close to that of the ideal antenna up to the angle of 80 deg (Fig. 3). The multipath error increase at the angles higher than 80 deg is caused by finiteness of the RP slope.

Thus, both the antennas with high RP slope and antennas with high polarization decoupling at the transition to the non-working angle range ($\theta > 90$ deg) are resistant to the multipath interference. The efficiency factor of the high-precision antennas is to be close to 100%. In terms of the accomplished studies, the promising antennas for the ground-based GNSS segment are those of the helical type. Directions of further research are associated with solving the problem of matching the helical antenna and analyzing accuracy characteristics in the entire GNSS frequency range.

Financial support

The study was supported by the Krasnoyarsk Region Foundation for Research and Technological Activities (project № 2021101507823 „GLONASS ground-based antennas for Far North regions "and project № 2022030108251 „Improvement of mid-wave radio navigation systems").

Conflict of interests

The authors declare that they have no conflict of interests.

References

[1] D.V. Tatarnikov, A.A. Generalov, *in Proc. of the Progress in Electromagnetics Research Symp.* (*PIERS*) (St. Petersburg, 2017), p. 800. DOI: 10.1109/PIERS.2017.8261851

[2] E.R. Gafarov, A.V. Stankovsky, Yu.P. Salomatov, in *2017 Radiation and scattering of electromagnetic waves* (*RSEMW*) (IEEE, 2017), p. 311. DOI: 10.1109/RSEMW.2017.8103659

[3] *Springer handbook of global navigation satellite systems*, ed. by P.J.G. Teunissen, O. Montenbruck (Springer International Publ., N.Y., 2017), p. 451.

[4] E.R. Gafarov, Yu.P. Salomatov, v sb. *Sistemy svyazi i radionavigatsii* (Krasnoyarsk, 2014), s. 102. (in Russian)

[5] M.K. Emara, J. Hautcoeur, G. Panther, J.S. Wight, S. Gupta, IEEE Trans. Antennas Propag., **67** (3), 2008 (2019). DOI: 10.1109/TAP.2019.2891553

[6] E.R. Gafarov, A.A. Erokhin, Yu.P. Salomatov, in *2019 Radiation and scattering of electromagnetic waves* (*RSEMW*) (IEEE, 2019), p. 128. DOI: 10.1109/RSEMW.2019.8792704

[7] D.V. Tatarnikov, A.P. Stepanenko, A.V. Astakhov, *in Proc. of the Progress in Electromagnetics Research Symp.* (*PIERS*) (St. Petersburg, 2017), p. 479. DOI: 10.1109/PIERS.2017.8261789

[8] A. Leick, L. Rapoport, D. Tatarnikov, *GPS satellite surveying* (John Wiley & Sons, Inc., Hoboken, 2015), p. 578–600.

[9] T. Meissner, F.J. Wentz, IEEE Trans. Geosci. Remote Sens., **42** (9), 1836 (2004). DOI: 10.1109/TGRS.2004.831888